Submitted to the
International Europhysics Conference on High Energy Physics
July 17 - 23, 2003, Aachen, Germany

Abstract: 564 **Sessions: HQCD, HP, HF**

Measurement of charm fragmentation ratios and fractions in γp collisions at HERA

ZEUS Collaboration

Abstract

The production of $D^{*\pm}$, D^0, $D^\pm$, $D_s^\pm$ and $\Lambda_c^\pm$ charm hadrons in γp collisions at HERA has been measured with the ZEUS detector using an integrated luminosity of $79\,\text{pb}^{-1}$. The measurement has been performed for photon-proton centre-of-mass energies in the range $130 < W < 300\,\text{GeV}$ and photon virtuality $Q^2 < 1\,\text{GeV}^2$. Charm hadrons have been reconstructed in the kinematic range $p_T(D, \Lambda_c) > 3.8\,\text{GeV}$ and $|\eta(D, \Lambda_c)| < 1.6$. The measured production cross sections have been used to determine the ratio of neutral and charged D meson production rates, $R_{u/d}$, the strangeness suppression factor, γ_s, and the fraction of D mesons produced in a vector state, P_v. The fractions of c quarks hadronising as a particular charm hadron, $f(c \rightarrow D, \Lambda_c)$, have been calculated in the accepted kinematic range. The results are compared with previous measurements.

1 Introduction

Charm quark production has been extensively studied at HERA using $D^{*\pm}$ and $D_s^{\pm}$ mesons [1–5]. The data have been compared with the theoretical predictions by assuming the universality of charm fragmentation. This assumption allows the charm fragmentation characteristics, obtained in e^+e^- annihilations, to be used in calculations of charm production in ep scattering. Measuring the charm fragmentation characteristics at HERA permits the verification of the charm-fragmentation universality and contributes to the knowledge of charm fragmentation.

This paper presents the measurement of the production of the weakly decaying charm ground states: D^0, $D^{\pm}$, $D_s^{\pm}$ pseudo-scalar mesons and $\Lambda_c^{\pm}$ baryons. The production of the charm vector meson $D^{*\pm}$ has also been studied. The measurement has been performed in ep scattering at HERA in the photoproduction regime ($Q^2 \approx 0$) for photon-proton centre-of-mass energies in the range $130 < W < 300\,\text{GeV}$. The measured production cross sections have been used to determine the ratio of neutral and charged D meson production rates, $R_{u/d}$, the strangeness suppression factor, γ_s, and the fraction of D mesons produced in a vector state, P_{v}. The fractions of c quarks hadronising as a particular charm hadron, $f(c \to D, \Lambda_c)$, have been calculated in the accepted kinematic range. The results are compared with those obtained in charm production in e^+e^- annihilations [6–9] and also in deep inelastic scattering (DIS) at HERA [10].

2 Event selection

The analysis was performed with data taken by the ZEUS Collaboration from 1998 to 2000. In this period, HERA collided positrons or electrons with energy $E_e = 27.56\,\text{GeV}$ and protons with energy $E_p = 920.0\,\text{GeV}$. The results are based on a sum of the e^-p and e^+p samples corresponding to a total integrated luminosity of $79.1 \pm 1.7\,\text{pb}^{-1}$. Due to trigger availability, the $D^{\pm}$ and $\Lambda_c^{\pm}$ production was measured using only the e^+p sample corresponding to an integrated luminosity of $65.5 \pm 1.5\,\text{pb}^{-1}$.

The ZEUS detector is described in detail elsewhere [11]. The major components of importance to this analysis are the uranium-scintillator calorimeter (CAL) [12], the central tracking detector (CTD) [13] and the luminosity monitor [14]. A three-level trigger system was used to select events online [11, 15].

Photoproduction events were selected by requiring that no scattered positron was identified in the CAL [16]. The Jacquet-Blondel [17] estimator of W, $W_{JB} = \sqrt{2E_p(E - p_Z)}$, was used[1], where $E - p_Z = \Sigma_i (E - p_Z)_i$ and the sum i runs over a combination of charged tracks, as measured in CTD, and energy clusters measured in the CAL [18]. After correcting for detector effects, the most important of which were energy losses in inactive material in front of the CAL and particle losses in the beam pipe [16, 19], events were selected in the interval $130 < W < 300\,\text{GeV}$. The lower limit was set by the trigger requirements, while the upper limit was imposed to suppress remaining events from deep inelastic scattering that have an unidentified scattered positron in the CAL [16]. Under these conditions, the photon virtuality, Q^2, lies below $1\,\text{GeV}^2$. The median Q^2 value was estimated from a Monte Carlo (MC) simulation to be about $3 \times 10^{-4}\,\text{GeV}^2$.

3 Reconstruction of charm hadrons

The production of $D^{*\pm}$, D^0, $D^\pm$, $D_s^\pm$ and $\Lambda_c^\pm$ charm hadrons was measured in the kinematic range $p_T(D, \Lambda_c) > 3.8\,\text{GeV}$ and $|\eta(D, \Lambda_c)| < 1.6$. Charm hadrons were reconstructed using tracks measured in the CTD and assigned to the reconstructed event vertex. The combinatorial background was much reduced by requiring $p_T(D)/E_T^{\theta>10^\circ} > 0.2$ and $p_T(\Lambda)/E_T^{\theta>10^\circ} > 0.25$ for charm mesons and baryons, respectively. The transverse energy was calculated as $E_T^{\theta>10^\circ} = \Sigma_{i,\theta_i>10^\circ}(E_i \sin\theta_i)$, where the sum runs over all energy deposits in the CAL with the polar angle outside a cone of $\theta = 10^\circ$ in the forward direction.

3.1 Reconstruction of D^0 mesons

The D^0 mesons were reconstructed from the decay channel $D^0 \to K^-\pi^+$ (+c.c.). In each event, tracks with opposite charges and transverse momenta $p_T > 0.8\,\text{GeV}$ were combined in pairs to form D^0 candidates. The nominal kaon and pion masses were assumed in turn for each track and the pair invariant mass, $M(K\pi)$, was calculated. The distribution of the cosine of the D^0 decay angle (defined as the angle $\theta^*(K)$ between the kaon in the $K\pi$ rest frame and the $K\pi$ line of flight in the laboratory) is isotropic, whereas the combinatorial background peaks forward and backward. To suppress the background, a cut $|\cos\theta^*(K)| < 0.85$ was applied.

[1] The ZEUS coordinate system is a right-handed Cartesian system, with the Z axis pointing in the proton beam direction, referred to as the "forward direction", and the X axis pointing left towards the centre of HERA. The coordinate origin is at the nominal interaction point. The pseudorapidity is defined as $\eta = -\ln\left(\tan\frac{\theta}{2}\right)$, where the polar angle, θ, is measured with respect to the proton beam direction.

For selected D^0 candidates, a search was performed for a track that could be a "soft" pion (π_s) in a $D^{*+} \to D^0\pi_s^+$ (+ c.c.) decay. The soft pion was required to have $p_T > 0.2\,\text{GeV}$ and a charge opposite to that of the particle taken as a kaon. The corresponding D^0 candidate was assigned to a class of candidates "with ΔM tag" if the mass difference, $\Delta M = M(K\pi\pi_s) - M(K\pi)$, was in the range $0.143 < \Delta M < 0.148\,\text{GeV}$. All remaining D^0 candidates were assigned to a class of candidates "without ΔM tag". For D^0 candidates with ΔM tag, the kaon and pion mass assignment was fixed by the track-charge requirements. For D^0 mesons without ΔM tag, the kaon and pion masses can be assigned to two tracks either correctly, producing a signal peak, or incorrectly, producing a wider reflected signal. To remove this reflection the mass distribution, obtained for D^0 candidates with ΔM tag and an opposite mass assignment to the kaon and pion tracks, was subtracted from the $M(K\pi)$ distribution for all D^0 candidates without ΔM tag. The subtracted mass distribution was normalised to the ratio of numbers of D^0 mesons without and with ΔM tag obtained from a fit described below.

Figure 1 shows the $M(K\pi)$ distribution for D^0 candidates without ΔM tag, obtained after the reflection subtraction, and the $M(K\pi)$ distribution for D^0 candidates with ΔM tag. Clear signals are seen at the nominal value of $M(D^0)$ in both distributions. The distributions were fitted simultaneously assuming the same shape for signals in both distributions. To describe the shape, a "modified" Gaussian function was used:

$$\text{Gauss}^{\text{mod}} \propto \exp[-0.5 \cdot x^{1+\frac{1}{1+0.5\cdot x}}],$$

where $x = |[M(K\pi) - M_0]/\sigma|$. The signal position, M_0, and width, σ, as well as the numbers of D^0 mesons in each signal were free parameters of the fit. Monte Carlo (MC) studies showed that background shapes in both distributions are compatible with linear in the ranges above the signals. Below the signals, the background shapes exhibit an exponential enhancement due to contributions from other D^0 decay modes and other D mesons. Therefore the background shape in the fit was described by the form $(A+B\cdot x)$ for $x > 1.86\,\text{GeV}$ and $(A+B\cdot x)\cdot\exp[C\cdot(x-1.86)]$ for $x < 1.86\,\text{GeV}$. The free parameters A, B and C were assumed to be independent for the two $M(K\pi)$ distributions. The numbers of D^0 mesons yielded by the fit were $N^{\text{untag}}(D^0) = 11370 \pm 560$ and $N^{\text{tag}}(D^0) = 3319 \pm 91$ for selections without and with ΔM tag, respectively.

3.2 Reconstruction of "additional" $D^{*\pm}$ mesons

The $D^{*+} \to D^0\pi_s^+$ (+ c.c.) events with $P_T(D^{*\pm}) > 3.8\,\text{GeV}$ and $|\eta(D^{*\pm})| < 1.6$ can be considered as a sum of two subsamples: events with a D^0 having $P_T(D^0) > 3.8\,\text{GeV}$ and $|\eta(D^0)| < 1.6$, and events with a D^0 outside of that kinematic range. The former sample is represented by D^0 mesons reconstructed with ΔM tag, as discussed in the previous section. The latter sample of "additional" $D^{*\pm}$ mesons was obtained using the same $D^0 \to K^-\pi + (+c.c.)$ decay channel and an independent selection described below.

In each event, tracks with opposite charges and transverse momenta $p_T > 0.4\,\mathrm{GeV}$ were combined in pairs to form D^0 candidates. To calculate the pair invariant mass, $M(K\pi)$, kaon and pion masses were assumed in turn for each track. Only D^0 candidates which satisfy $1.81 < M(K\pi) < 1.92\,\mathrm{GeV}$ were kept. Moreover, the D^0 candidates were required to have $P_T(D^0) < 3.8\,\mathrm{GeV}$ or $|\eta(D^0)| < 1.6$. Any additional track, with $p_T > 0.2\,\mathrm{GeV}$ and a charge opposite to that of the kaon track, was assigned the pion mass and combined with the D^0 candidate to form a $D^{*\pm}$ candidate with invariant mass $M(K\pi\pi_s)$.

Figure 2 shows the distribution of the mass difference, $\Delta M = M(K\pi\pi_s) - M(K\pi)$, for the $D^{*\pm}$ candidates after all cuts. A clear signal is seen at the nominal value of $M(D^{*\pm}) - M(D^0)$. The combinatorial background under this signal was estimated from the mass-difference distribution for wrong-charge combinations, in which both tracks forming the D^0 candidates have the same charge and the third track has the opposite charge. The number of reconstructed "additional" $D^{*\pm}$ mesons was determined by subtracting the wrong-charge ΔM distribution after normalising it to the distribution of $D^{*\pm}$ candidates with the appropriate charges in the range $0.15 < \Delta M < 0.17\,\mathrm{GeV}$. The subtraction, performed in the signal range $0.143 < \Delta M < 0.148\,\mathrm{GeV}$, yielded $N^{\mathrm{add}}(D^{*\pm}) = 889 \pm 41$.

3.3 Reconstruction of $D^\pm$ mesons

The $D^\pm$ mesons were reconstructed from the decay channel $D^+ \to K^-\pi^+\pi^+$ (+c.c.). In each event, two tracks with the same charges and $p_T > 0.5\,\mathrm{GeV}$ and a third track with opposite charge and $p_T > 0.7\,\mathrm{GeV}$ were combined to form $D^\pm$ candidates. The pion masses were assigned to the two tracks with the same charges and the kaon mass was assigned to the third track, after which the candidate invariant mass, $M(K\pi\pi)$, was calculated. To suppress the combinatorial background, a cut of $\cos\theta^*(K) > -0.75$ was imposed, where $\theta^*(K)$ is the angle between the kaon in the $K\pi\pi$ rest frame and the $K\pi\pi$ line of flight in the laboratory.

Figure 3 shows the $M(K\pi\pi)$ distribution for the $D^\pm$ candidates after all cuts. A clear signal is seen at the nominal value of $M(D^+)$. The mass distribution was fitted to a sum of a modified Gaussian function describing the signal and a linear function describing the non-resonant background. The number of reconstructed $D^\pm$ mesons yielded by the fit was $N(D^\pm) = 9600 \pm 620$.

3.4 Reconstruction of $D_s^{\pm}$ mesons

The $D_s^{\pm}$ mesons were reconstructed from the decay channels $D_s^+ \to \phi\pi^+$ with $\phi \to K^+K^-$ (+c.c.). In each event, tracks with opposite charges and $p_T > 0.7$ GeV were assigned the kaon mass and combined in pairs to form ϕ candidates. The ϕ candidate was kept if its invariant mass, $M(KK)$, was within ± 8 MeV of the nominal ϕ mass [4]. Any additional track with $p_T > 0.5$ GeV was assigned the pion mass and combined with the ϕ candidate to form a $D_s^{\pm}$ candidate with invariant mass $M(KK\pi)$. To suppress the combinatorial background, two requirements were applied:

- $|\cos^3\theta^{**}(K)| > 0.1$, where $\theta^{**}(K)$ is the angle between one of the kaons and the pion in the KK rest frame. The use of this cut was discussed in the previous ZEUS publication [4];
- $\cos\theta^*(\pi) < 0.85$, where $\theta^*(\pi)$ is the angle between the pion in the $KK\pi$ rest frame and the $KK\pi$ line of flight in the laboratory.

Figure 4 shows the $M(KK\pi)$ distribution for the $D_s^{\pm}$ candidates after all cuts. A clear signal is seen at the nominal value of $M(D_s^+)$. There is also a smaller signal around the nominal value of $M(D^+)$ as expected from the decay channels $D^+ \to \phi\pi^+$ with $\phi \to K^+K^-$ (+c.c.). The mass distribution was fitted to a sum of two modified Gaussian functions describing the signals and an exponential function describing the non-resonant background. The numbers of reconstructed $D_s^{\pm}$ and $D^{\pm}$ mesons yielded by the fit were $N(D_s^{\pm}) = 1086 \pm 85$ and $N(D^{\pm}) = 229 \pm 62$, respectively. Only the number of reconstructed $D_s^{\pm}$ mesons was used for calculations of charm fragmentation ratios and fractions.

3.5 Reconstruction of $\Lambda_c^{\pm}$ baryons

The $\Lambda_c^{\pm}$ baryons were reconstructed from the decay channel $\Lambda_c^+ \to K^-p\pi^+$ (+c.c.). In each event, two tracks with the same charges and a third track with opposite charge were combined to form $\Lambda_c^{\pm}$ candidates. Due to a large difference between the proton and pion masses, the proton momentum in the laboratory is typically larger than the momentum of the pion from the decay. Therefore, the proton (pion) mass was assigned to those of the two tracks with the same charges which had larger (smaller) momentum. The kaon mass was assigned to the third track and the candidate invariant mass, $M(Kp\pi)$, was calculated. Only candidates with $p_T(K) > 0.6$ GeV, $p_T(p) > 0.8$ GeV and $p_T(\pi) > 0.5$ GeV were kept. To suppress the combinatorial background, the following requirements, motivated by MC studies, were applied:

- $-0.9 < cos\theta^*(K) < 0.75$, where $\theta^*(K)$ is the angle between the kaon in the $Kp\pi$ rest frame and the $Kp\pi$ line of flight in the laboratory;

- $-0.8 < cos\theta^*(p) < 0.85$, where $\theta^*(p)$ is the angle between the proton in the $Kp\pi$ rest frame and the $Kp\pi$ line of flight in the laboratory;
- $p^*(\pi) > 90\,\mathrm{MeV}$, where $p^*(\pi)$ is the pion momentum in the $Kp\pi$ rest frame.

Figure 5 shows the $M(Kp\pi)$ distribution for the $\Lambda_c^\pm$ candidates after all cuts. A clear signal is seen at the nominal value of $M(\Lambda_c^+)$. The mass distribution was fitted to a sum of a modified Gaussian function describing the signal and a linear function describing the non-resonant background. The number of reconstructed $\Lambda_c^\pm$ baryons yielded by the fit was $N(\Lambda_c^\pm) = 1390 \pm 380$.

4 Charm fragmentation ratios and fractions

4.1 Charm hadron production cross sections

The inclusive charm hadron cross sections were calculated for the process $ep \to eD(\Lambda_c)X$ in the kinematic region $Q^2 < 1\,\mathrm{GeV}^2$, $130 < W < 300\,\mathrm{GeV}$, $p_T(D,\Lambda_c) > 3.8\,\mathrm{GeV}$ and $|\eta(D,\Lambda_c)| < 1.6$. The cross section for a given charm hadron was calculated from

$$\sigma(D,\Lambda_c) = \frac{N(D,\Lambda_c)}{A \cdot \mathcal{L} \cdot B},$$

where $N(D,\Lambda_c)$ is the number of reconstructed charm hadrons, A is the acceptance for this charm hadron, $\mathcal{L}$ is the integrated luminosity and B is the branching ratio or the product of the branching ratios [20] for the decay channel used in the reconstruction. Using the reconstructed signals (Section 3) the following cross sections were calculated:

- $\sigma^{\mathrm{untag}}(D^0)$, the production cross section for D^0 mesons not originating from the $D^{*+} \to D^0\pi_s^+$ (+ c.c.) decays;
- $\sigma^{\mathrm{tag}}(D^0)$, the production cross section for D^0 mesons originating from the $D^{*+} \to D^0\pi_s^+$ (+ c.c.) decays. The ratio $\sigma^{\mathrm{tag}}(D^0)/B_{D^{*+}\to D^0\pi^+}$ gives that part of the $D^{*\pm}$ inclusive cross section which corresponds to D^0 production with $p_T(D^0) > 3.8\,\mathrm{GeV}$ and $|\eta(D^0)| < 1.6$ in case of the $D^{*+} \to D^0\pi_s^+$ (+ c.c.) decay. Here $B_{D^{*+}\to D^0\pi^+} = 0.677 \pm 0.005$ [20] is the branching ratio of the $D^{*+} \to D^0\pi_s^+$ decay;
- $\sigma^{\mathrm{add}}(D^{*\pm})$, the "additional" production cross section for $D^{*\pm}$ mesons. The sum $\sigma^{\mathrm{add}}(D^{*\pm}) + \sigma^{\mathrm{tag}}(D^0)/B_{D^{*+}\to D^0\pi^+}$ gives the inclusive production cross section for $D^{*\pm}$ mesons with $p_T(D^{*\pm}) > 3.8\,\mathrm{GeV}$ and $|\eta(D^{*\pm})| < 1.6$;
- $\sigma(D^\pm)$, the production cross section for $D^\pm$ mesons;
- $\sigma(D_s^\pm)$, the production cross section for $D_s^\pm$ mesons;
- $\sigma(\Lambda_c^\pm)$, the production cross section for $\Lambda_c^\pm$ baryons.

The MC samples of charm and beauty events used for the acceptance calculations were produced with the PYTHIA 6.156 [21], RAPGAP 2.0818 [22] and HERWIG 6.301 [23] generators. The generation included direct photon processes, in which the photon couples directly to a parton in the proton, and resolved photon processes, where the photon acts as a source of partons, one of which participates in the hard scattering process. The CTEQ5L [24] and GRV LO [25] parametrisations were used for the proton and photon structure functions, respectively. The quark masses were set to the values $m_c = 1.5\,\mathrm{GeV}$ and $m_b = 4.75\,\mathrm{GeV}$. All components were generated proportionally to the predicted MC cross sections. The MC events were processed through the standard ZEUS detector- and trigger-simulation programs and event reconstruction package.

The combined sample of the PYTHIA events, generated with $Q^2 < 0.6\,\mathrm{GeV}^2$, and the RAPGAP events, generated with $Q^2 > 0.6\,\mathrm{GeV}^2$, was used to evaluate the nominal acceptances. The b-quark relative contribution, predicted by the MC simulation, was subtracted from all measured cross sections. This b-quark fraction was varied by a factor of two when evaluating systematic uncertainties. The HERWIG MC sample was used to estimate the model dependence of the acceptance corrections. The uncertainties originating from the signal extraction procedure and the tracking simulation were also considered. Common systematic uncertainties, producing the same effect on all measured cross sections, are cancelled in the calculation of the fragmentation ratios and fractions. Contributions from the different systematic uncertainties were calculated and added in quadrature separately for positive and negative variations.

The uncertainties due to the branching ratios [20], which are small for the non-strange charm mesons and larger for $D_s^\pm$ and $\Lambda_c^\pm$, were not included in the systematic errors. These uncertainties can be ignored in the comparison with other measurements based on the same charm-hadron decay channels.

4.2 Ratio of neutral and charged D meson production rates

Neglecting distortions from decays of excited D mesons with non-zero orbital angular momentum, the ratio of neutral and charged D meson production rates is given by the ratio of the sum of D^{*0} and direct D^0 production cross sections to the sum of $D^{*\pm}$ and direct $D^\pm$ production cross sections. The direct D^0 and $D^\pm$ production cross sections are those parts of their inclusive cross sections which do not originate from D^{*0} and $D^{*\pm}$ decays. Thus, since all D^{*0} decays produce a D^0 meson [20], the ratio is given by

$$R_{u/d} = \frac{\sigma(D^0) - \sigma(D^{*\pm}) \times B_{D^{*+}\to D^0\pi^+}}{\sigma(D^\pm) - \sigma(D^{*\pm}) \times (1 - B_{D^{*+}\to D^0\pi^+}) + \sigma(D^{*\pm})} = \frac{\sigma(D^0) - \sigma(D^{*\pm}) \times B_{D^{*+}\to D^0\pi^+}}{\sigma(D^\pm) + \sigma(D^{*\pm}) \times B_{D^{*+}\to D^0\pi^+}}.$$

Replacing $\sigma(D^{*\pm}) \times B_{D^{*+}\to D^0\pi^+}$ with $\sigma^{\rm tag}(D^0)$ and $\sigma(D^0) - \sigma^{\rm tag}(D^0)$ with $\sigma^{\rm untag}(D^0)$ gives

$$R_{u/d} = \frac{\sigma^{\rm untag}(D^0)}{\sigma(D^{\pm}) + \sigma^{\rm tag}(D^0)}.$$

Using the measured cross sections, the ratio of neutral and charged D meson production rates, obtained for the kinematic region $Q^2 < 1\,\text{GeV}^2$, $130 < W < 300\,\text{GeV}$, $p_T(D) > 3.8\,\text{GeV}$ and $|\eta(D)| < 1.6$, is

$$R_{u/d} = 1.014 \pm 0.068\,(\text{stat})^{+0.024}_{-0.031}\,(\text{syst}).$$

The measured $R_{u/d}$ value agrees with one. This confirms isospin invariance which suggests u and d quarks are produced equally in charm fragmentation.

Table 1 compares the measurement with the value obtained in deep inelastic scattering [10] and with those from e^+e^- annihilations [6–8]. All measurements agree with one within experimental uncertainties.

With isospin invariance thus confirmed, the production rates of D^{*0} and D^{*+} mesons are assumed to be equal in the following. In addition, the inclusive production cross sections for D^0 and $D^{\pm}$ mesons will be replaced by the sums of their direct cross sections and contributions from D^* decays. The latter contributions will be calculated from the $D^{*\pm}$ meson cross section measured for $p_T(D^{*\pm}) > 3.8\,\text{GeV}$ and $|\eta(D^{*\pm})| < 1.6$. MC studies show that such "equivalent phase space treatment" for the non-strange D and D^* mesons minimises differences between the fragmentation ratios and fractions measured in the accepted $p_T(D, \Lambda_c)$ and $\eta(D, \Lambda_c)$ kinematic region and those in the full phase space.

4.3 Strangeness suppression factor

Neglecting distortions from decays of excited D mesons with non-zero orbital angular momentum, the strangeness suppression factor is given by

$$\gamma_s = \frac{2\,\sigma(D_s^{\pm})}{\sigma(D^{\pm}) + \sigma(D^0)}.$$

Applying the equivalent phase space treatment gives

$$\gamma_s = \frac{2\,\sigma(D_s^{\pm})}{\sigma(D^{\pm}) + \sigma^{\rm untag}(D^0) + \sigma^{\rm tag}(D^0) + 2\,\sigma^{\rm add}(D^{*\pm})}.$$

Using the measured cross sections, the strangeness suppression factor, obtained for the kinematic region $Q^2 < 1\,\text{GeV}^2$, $130 < W < 300\,\text{GeV}$, $p_T(D) > 3.8\,\text{GeV}$ and $|\eta(D)| < 1.6$, equals

$$\gamma_s = 0.266 \pm 0.023\,(\text{stat})^{+0.014}_{-0.012}\,(\text{syst}).$$

Thus, the s quark production is suppressed by a factor ≈ 3.5 in charm fragmentation.

Table 2 compares the measurement with the previous ZEUS 96-97 result, calculated from the ratio of $D_s^\pm$ to $D^{*\pm}$ cross sections [4], and with the values obtained for charm production in deep inelastic scattering (DIS) [10] and in e^+e^- annihilations. The latter value was calculated as $2f(c \to D_s^+)/[f(c \to D^+) + f(c \to D^0)]$ using fragmentation fractions from [9]. All measurements agree within experimental uncertainties.

4.4 Fraction of D mesons produced in a vector state

Neglecting distortions from decays of excited D mesons with non-zero orbital angular momentum, the fraction of D mesons produced in a vector state is given by the ratio of vector/(vector+pseudoscalar) charm meson production cross sections. Only direct parts of the production cross sections for pseudoscalar charm mesons should be used. Applying the equivalent phase space treatment, the fraction for charged charm mesons is given by

$$P_{\rm v}^d = \frac{\sigma^{\rm tag}(D^0)/B_{D^{*+}\to D^0\pi^+} + \sigma^{\rm add}(D^{*\pm})}{\sigma(D^\pm) + \sigma^{\rm tag}(D^0) + \sigma^{\rm add}(D^{*\pm})}.$$

Using the measured cross sections, the fraction of charged D mesons produced in a vector state, obtained for the kinematic region $Q^2 < 1\,{\rm GeV}^2$, $130 < W < 300\,{\rm GeV}$, $p_T(D) > 3.8\,{\rm GeV}$ and $|\eta(D)| < 1.6$, is

$$P_{\rm v}^d = 0.557 \pm 0.023\,({\rm stat})^{+0.009}_{-0.006}\,({\rm syst}).$$

Assuming the same production rates for the D^{*0} and D^{*+} mesons, the fraction of D mesons produced in a vector state can be calculated for the sum of charged and neutral charm mesons:

$$P_{\rm v} = \frac{2\,\sigma^{\rm tag}(D^0)/B_{D^{*+}\to D^0\pi^+} + 2\,\sigma^{\rm add}(D^{*\pm})}{\sigma(D^\pm) + \sigma^{\rm untag}(D^0) + \sigma^{\rm tag}(D^0) + 2\,\sigma^{\rm add}(D^{*\pm})}.$$

Using the measured cross sections, the fraction for the sum of charged and neutral charm mesons, obtained for the kinematic region $Q^2 < 1\,{\rm GeV}^2$, $130 < W < 300\,{\rm GeV}$, $p_T(D) > 3.8\,{\rm GeV}$ and $|\eta(D)| < 1.6$, is

$$P_{\rm v} = 0.554 \pm 0.019\,({\rm stat})^{+0.008}_{-0.004}\,({\rm syst}).$$

The fraction can be also calculated for charged vector mesons ($D^{*\pm}$) and neutral pseudoscalar mesons (D^0):

$$P_{\rm v}^{d/u} = \frac{\sigma^{\rm tag}(D^0)/B_{D^{*+}\to D^0\pi^+} + \sigma^{\rm add}(D^{*\pm})}{\sigma^{\rm untag}(D^0) + \sigma^{\rm add}(D^{*\pm})}.$$

Using the measured cross sections, the fraction, calculated for charged vector charm mesons and neutral pseudoscalar charm mesons in the kinematic region $Q^2 < 1\,\mathrm{GeV}^2$, $130 < W < 300\,\mathrm{GeV}$, $p_T(D) > 3.8\,\mathrm{GeV}$ and $|\eta(D)| < 1.6$, is

$$P_{\rm v}^{d/u} = 0.551 \pm 0.027(\mathrm{stat})^{+0.014}_{-0.006}(\mathrm{syst}).$$

The measured $P_{\rm v}^{d/u}$ is in good agreement with our previous preliminary measurement [26] and supersedes it.

The measured $P_{\rm v}^{d}$, $P_{\rm v}$ and $P_{\rm v}^{d/u}$ fractions are sizeably smaller than the naive spin counting prediction of 0.75. The predictions of the thermodynamical approach [27] and the string fragmentation approach [28], which both predict 2/3 for the fraction, are closer to, but still above, the measured value.

Table 3 compares the measurement with the value obtained in deep inelastic scattering (DIS) [10] and with those from e^+e^- annihilations [6–8]. All measurements agree within experimental uncertainties.

4.5 Charm fragmentation fractions

The fraction of c quarks hadronising as a particular charm hadron, $f(c \to D, \Lambda_c)$, is given by the ratio of the production cross section for the hadron to the sum of the production cross sections for all charm weakly-decaying ground states. In addition to the measured D^0, $D^\pm$, $D_s^\pm$ and $\Lambda_c^\pm$ charm ground states, the strange-charm baryons $\Xi_c^\pm$, Ξ_c^0 and Ω_c^0 production cross sections should be included in the sum. The production rates for these baryons are expected to be much lower than that of the $\Lambda_c^\pm$ due to strangeness suppression. The relative rates for the weakly decaying strange-charm baryons were estimated from the non-charm sector as in [29]. The measured $\Xi^\pm/\Lambda$ and $\Omega^\pm/\Lambda$ relative rates are $(6.65 \pm 0.28)\%$ and $(0.42 \pm 0.07)\%$, respectively [20]. Assuming equal production of Ξ^0 and $\Xi^\pm$ states and that a similar suppression is applicable to the charm baryons, the total rate for the three strange-charm baryons relative to the $\Lambda_c^\pm$ state is expected to be about 14%. Therefore the $\Lambda_c^\pm$ production cross section was scaled by the factor 1.14 in the sum of the production production cross sections. The error of ± 0.05 was assigned to the scale factor when evaluating systematic uncertainties.

Applying the equivalent phase space treatment, the sum of the production cross sections for all charm ground states (g.s.) is given by

$$\sum_{\rm all} \sigma_{\rm g.s.} = \sigma(D^\pm) + \sigma^{\rm untag}(D^0) + \sigma^{\rm tag}(D^0) + 2\,\sigma^{\rm add}(D^{*\pm}) + \sigma(D_s^\pm) + \sigma(\Lambda_c^\pm) \times 1.14$$

Using this sum, the fragmentation fractions for the measured charm hadrons are given by

$$f(c \to D^+) = [\sigma(D^\pm) + \sigma^{\rm add}(D^{*\pm}) * (1 - B_{D^{*+}\to D^0\pi^+})] / \sum_{\rm all} \sigma_{\rm g.s.}$$

$$f(c \to D^0) = [\sigma^{\mathrm{untag}}(D^0) + \sigma^{\mathrm{tag}}(D^0) + \sigma^{\mathrm{add}}(D^{*\pm}) * (1 + B_{D^{*+}\to D^0\pi^+})] / \sum_{\mathrm{all}} \sigma_{\mathrm{g.s.}}$$

$$f(c \to D_s^+) = \sigma(D_s^\pm) / \sum_{\mathrm{all}} \sigma_{\mathrm{g.s.}}$$

$$f(c \to \Lambda_c^+) = \sigma(\Lambda_c^\pm) / \sum_{\mathrm{all}} \sigma_{\mathrm{g.s.}}$$

$$f(c \to D^{*+}) = [\sigma^{\mathrm{tag}}(D^0)/B_{D^{*+}\to D^0\pi^+} + \sigma^{\mathrm{add}}(D^{*\pm})] / \sum_{\mathrm{all}} \sigma_{\mathrm{g.s.}}$$

The measured fragmentation fractions are compared in Table 4 with the values obtained for charm production in e^+e^- annihilations [9] and in deep inelastic scattering (DIS) [10]. All measurements agree within experimental uncertainties. This confirms the universality of charm fragmentation.

4.6 Discussion of extrapolation effects

The charm fragmentation ratios and fractions were measured in the region $p_T(D, \Lambda_c) > 3.8\,\mathrm{GeV}$ and $|\eta(D, \Lambda_c)| < 1.6$. To minimise differences between the values measured in the accepted $p_T(D, \Lambda_c)$ and $\eta(D, \Lambda_c)$ kinematic region and those in the full phase space, the equivalent phase space treatment for the non-strange D and D^* mesons was used (see Section 4.2).

Table 5 shows estimations of the extrapolation factors correcting the values measured in the accepted $p_T(D, \Lambda_c)$ and $\eta(D, \Lambda_c)$ region to those in the full phase space. The estimations were performed using three fragmentation schemes: the Peterson parameterisation [30] of the charm fragmentation function as implemented in PYTHIA, the Bowler modification [31] of the LUND symmetric fragmentation function [32] as implemented in PYTHIA and the cluster model [33] as implemented in HERWIG. The quoted uncertainties were obtained by varying relevant parameters in the PYTHIA and HERWIG MC generators. The extrapolation factors obtained are generally close to 1.0. The only exceptions are the correction factors, predicted by the cluster model, for the $f(c \to \Lambda_c^+)$ and, to a lesser extent, for the γ_s and $f(c \to D_s^+)$ values.

This MC study suggests that the measured charm fragmentation ratios and fractions are close to those in the full $p_T(D, \Lambda_c)$ and $\eta(D, \Lambda_c)$ phase space. A good agreement of our measured values with other measurements extrapolated to the full phase space [4, 6–10] supports this expectation.

5 Summary

The production of $D^{*\pm}$, D^0, $D^\pm$, $D_s^\pm$ and $\Lambda_c^\pm$ charm hadrons has been measured with the ZEUS detector in the kinematic range $p_T(D,\Lambda_c) > 3.8\,\text{GeV}$ and $|\eta(D,\Lambda_c)| < 1.6$, $130 < W < 300\,\text{GeV}$ and $Q^2 < 1\,\text{GeV}^2$. The measured production cross sections have been used to determine in the above kinematic range the charm fragmentation ratios and fractions.

The ratio of neutral and charged D meson production rates has been measured to be

$$R_{u/d} = 1.014 \pm 0.068\,(\text{stat})^{+0.024}_{-0.031}\,(\text{syst}).$$

The measured $R_{u/d}$ value agrees with one. This confirms isospin invariance which suggests u and d quarks are produced equally in charm fragmentation.

The strangeness suppression factor has been measured to be

$$\gamma_s = 0.266 \pm 0.023\,(\text{stat})^{+0.014}_{-0.012}\,(\text{syst}).$$

Thus, the s quark production is suppressed by a factor $3-4$ in charm fragmentation.

The fraction of charged D mesons produced in a vector state has been measured to be

$$P_{\text{v}}^d = 0.557 \pm 0.023\,(\text{stat})^{+0.009}_{-0.006}\,(\text{syst}),$$

while the fraction for the sum of charged and neutral charm mesons is

$$P_{\text{v}} = 0.554 \pm 0.019\,(\text{stat})^{+0.008}_{-0.004}\,(\text{syst}).$$

The measured fractions are sizeably smaller than the naive spin counting prediction of 0.75. The predictions of the thermodynamical approach [27] and the string fragmentation approach [28], which both predict 2/3 for the fraction, are closer to, but still above, the measured value.

The fractions of c quarks hadronising as $D^{*\pm}$, D^0, $D^\pm$, $D_s^\pm$ and $\Lambda_c^\pm$ hadrons have been calculated in the accepted kinematic range.

All measured fragmentation characteristics agree with those obtained for charm production in e^+e^- annihilations, thus confirming the universality of charm fragmentation.

6 Acknowledgements

We would like to thank the DESY Directorate for their strong support and encouragement. The remarkable achievements of the HERA machine group were vital for the successful completion of this work and are greatly appreciated.

References

[1] ZEUS Coll., J. Breitweg et al., Eur. Phys. J. **C 6**, 67 (1999).

[2] H1 Coll., C. Adloff et al., Nucl. Phys. **B 545**, 21 (1999).

[3] ZEUS Coll., J. Breitweg et al., Eur. Phys. J. **C 12**, 35 (2000).

[4] ZEUS Coll., J. Breitweg et al., Phys. Lett. **B 481**, 213 (2000).

[5] H1 Coll., C. Adloff et al., Phys. Lett. **B 528**, 199 (2002).

[6] DELPHI Coll., P. Abreu et al., Eur. Phys. J. **C 12**, 225 (2000).

[7] ALEPH Coll., R. Barate et al., Eur. Phys. J. **C 16** (2000).

[8] OPAL Coll., K. Ackerstaff et al., Eur. Phys. J. **C 5**, 1 (1998).

[9] L. Gladilin, Preprint hep-ex/9912064, 1999.

[10] H1 Coll., *Measurement of Inclusive D-meson Production in Deep Inelastic Scattering at HERA*. Abstract 1015, 31st International Conference on High Energy Physics, Amsterdam, Netherlands, 2002, 2002.

[11] ZEUS Coll., U. Holm (ed.), *The ZEUS Detector*. Status Report (unpublished), DESY (1993), available on `http://www-zeus.desy.de/bluebook/bluebook.html`.

[12] M. Derrick et al., Nucl. Inst. Meth. **A 309**, 77 (1991);
A. Andresen et al., Nucl. Inst. Meth. **A 309**, 101 (1991);
A. Caldwell et al., Nucl. Inst. Meth. **A 321**, 356 (1992);
A. Bernstein et al., Nucl. Inst. Meth. **A 336**, 23 (1993).

[13] N. Harnew et al., Nucl. Inst. Meth. **A 279**, 290 (1989);
B. Foster et al., Nucl. Phys. Proc. Suppl. **B 32**, 181 (1993);
B. Foster et al., Nucl. Inst. Meth. **A 338**, 254 (1994).

[14] J. Andruszków et al., Preprint DESY-92-066, DESY, 1992;
ZEUS Coll., M. Derrick et al., Z. Phys. **C 63**, 391 (1994);
J. Andruszków et al., Acta Phys. Pol. **B 32**, 2025 (2001).

[15] W. H. Smith, K. Tokushuku and L. W. Wiggers, *Proc. Computing in High-Energy Physics (CHEP), Annecy, France, Sept. 1992*, C. Verkerk and W. Wojcik (eds.), p. 222. CERN, Geneva, Switzerland (1992). Also in preprint DESY 92-150B.

[16] ZEUS Coll., M. Derrick et al., Phys. Lett. **B 322**, 287 (1994).

[17] F. Jacquet and A. Blondel, *Proceedings of the Study for an ep Facility for Europe*, U. Amaldi (ed.), p. 391. Hamburg, Germany (1979). Also in preprint DESY 79/48.

[18] G.M. Briskin. Ph.D. Thesis, Tel Aviv University, 1998. (Unpublished).

[19] ZEUS Coll., M. Derrick et al., Phys. Lett. **B 349**, 225 (1995).

[20] Particle Data Group, K. Hagiwara et al., Phys. Rev. **D 66**, 10001 (2002).

[21] T. Sjöstrand, Comp. Phys. Comm. **82**, 74 (1994).

[22] H. Jung, Comp. Phys. Comm. **86**, 147 (1995).

[23] G. Marchesini et al., Comp. Phys. Comm. **67**, 465 (1992);
G. Corcella et al., JHEP **0101**, 010 (2001).

[24] CTEQ Coll., H.L. Lai et al., Eur. Phys. J. **C 12**, 375 (2000).

[25] M. Glück, E. Reya and A. Vogt, Phys. Rev. **D 46**, 1973 (1992).

[26] ZEUS Coll., *Study of Inclusive D^0 Photoproduction at HERA*. Abstract 501, *XXXth International Conference on High Energy Physics, Budapest, Hungary (EPS2001)*, July 2001, 2001, available on
`http://www-zeus.desy.de/physics/phch/conf/eps01_paper.html`.

[27] F. Becattini, Z. Phys. **C 69**, 485 (1996).

[28] Yi-Jin Pei, Z. Phys. **C 72**, 39 (1996).

[29] OPAL Coll., G. Alexander et al., Z. Phys. **C 72**, 1 (1996).

[30] C. Peterson et al., Phys. Rev. **D 27**, 105 (1983).

[31] M. G. Bowler, Z. Phys. **C 11**, 169 (1981).

[32] B. Andersson, G. Gustafson and B. Söderberg, Z. Phys. **C 20**, 317 (1983).

[33] B. R. Webber, Nucl. Phys. **B 238**, 492 (1984).

	$R_{u/d}$
ZEUS prel. (γp)	$1.014 \pm 0.068^{+0.024}_{-0.031}$
H1 prel. (DIS) [10]	$1.26 \pm 0.20 \pm 0.11 \pm 0.04$
DELPHI [6]	$0.963 \pm 0.051 \pm 0.054$
ALEPH [7]	1.02 ± 0.12
OPAL [8]	1.19 ± 0.36

Table 1: *The ratio of neutral and charged D meson production rates. The first and second uncertainties represent statistical and systematic uncertainties, respectively. The uncertainties due to the branching ratios are not included in the systematic errors. For the ALEPH and OPAL measurements, the combined statistical and systematic uncertainties are quoted. The third uncertainty, quoted for the H1 measurement, is due to the uncertainty of theoretical calculations used.*

	γ_s
ZEUS prel. (γp)	$0.266 \pm 0.023^{+0.014}_{-0.012}$
ZEUS 96-97 [4]	$0.27 \pm 0.04^{+0.02}_{-0.03}$
H1 prel. (DIS) [10]	$0.36 \pm 0.10 \pm 0.01 \pm 0.08$
e^+e^- annihilations [9]	0.26 ± 0.03

Table 2: *The strangeness suppression factor in charm fragmentation. The ZEUS 96-97 value was calculated from the ratio of $D_s^{\pm}$ to $D^{*\pm}$ cross sections. The first and second uncertainties represent statistical and systematic uncertainties, respectively. The uncertainties due to the branching ratios are not included in the systematic errors. For the value obtained for charm production in e^+e^- annihilations, the combined statistical and systematic uncertainty is quoted. The third uncertainty, quoted for the H1 measurement, is due to the uncertainty of theoretical calculations used.*

	$P_{\rm v}^d$	$P_{\rm v}$
ZEUS prel. (γp)	$0.557 \pm 0.023^{+0.009}_{-0.006}$	$0.554 \pm 0.019^{+0.008}_{-0.004}$
H1 prel. (DIS) [10]	$0.693 \pm 0.045 \pm 0.004 \pm 0.009$	$0.613 \pm 0.061 \pm 0.033 \pm 0.008$
DELPHI [6]		$0.620 \pm 0.014 \pm 0.014$
ALEPH [7]	0.595 ± 0.045	
OPAL [8]		0.57 ± 0.05

Table 3: *The fraction of D mesons produced in a vector state for charged charm mesons, $P_{\rm v}^d$, and for the sum of charged and neutral charm mesons, $P_{\rm v}$. The first and second uncertainties represent statistical and systematic uncertainties, respectively. The uncertainties due to the branching ratios are not included in the systematic errors. For the ALEPH and OPAL measurements, the combined statistical and systematic uncertainties are quoted. The third uncertainty, quoted for the H1 measurements, is due to the uncertainty of theoretical calculations used.*

	ZEUS prel. (γp) $p_T(D,\Lambda_c) > 3.8\,{\rm GeV}$ $\lvert\eta(D,\Lambda_c)\rvert < 1.6$	Combined e^+e^- data [9]	H1 prel. (DIS) [10]
$f(c \to D^+)$	$0.249 \pm 0.014^{+0.004}_{-0.008}$	0.232 ± 0.010	$0.202 \pm 0.020^{+0.045}_{-0.033}{}^{+0.029}_{-0.021}$
$f(c \to D^0)$	$0.557 \pm 0.019^{+0.005}_{-0.013}$	0.549 ± 0.023	$0.658 \pm 0.054^{+0.117}_{-0.142}{}^{+0.086}_{-0.048}$
$f(c \to D_s^+)$	$0.107 \pm 0.009 \pm 0.005$	0.101 ± 0.009	$0.156 \pm 0.043^{+0.036}_{-0.035}{}^{+0.050}_{-0.046}$
$f(c \to \Lambda_c^+)$	$0.076 \pm 0.020^{+0.017}_{-0.001}$	0.076 ± 0.007	
$f(c \to D^{*+})$	$0.223 \pm 0.009^{+0.003}_{-0.005}$	0.235 ± 0.007	$0.263 \pm 0.019^{+0.056}_{-0.042}{}^{+0.031}_{-0.022}$

Table 4: *The fractions of c quarks hadronising as a particular charm hadron. The first and second uncertainties represent statistical and systematic uncertainties, respectively. The uncertainties due to the branching ratios are not included in the systematic errors. For the values obtained for charm production in e^+e^- annihilations, the combined statistical and systematic uncertainties are quoted. The third uncertainty, quoted for the H1 measurements, is due to the uncertainty of theoretical calculations used.*

	Peterson (PYTHIA)	Bowler (PYTHIA)	Cluster model (HERWIG)
$R_{u/d}$	$0.99^{+0.02}_{-0.00}$	$0.99^{+0.02}_{-0.00}$	$1.00^{+0.01}_{-0.00}$
γ_s	$1.04^{+0.04}_{-0.07}$	$1.00^{+0.02}_{-0.00}$	$1.18^{+0.07}_{-0.05}$
$P_{\rm v}^d$	1.00 ± 0.02	$0.97^{+0.01}_{-0.00}$	$0.96^{+0.02}_{-0.01}$
$P_{\rm v}$	$1.00^{+0.01}_{-0.03}$	$0.97^{+0.00}_{-0.01}$	$0.96^{+0.02}_{-0.01}$
$P_{\rm v}^{d/u}$	$1.01^{+0.01}_{-0.04}$	$0.97^{+0.00}_{-0.02}$	0.96 ± 0.01
$f(c \to D^+)$	$1.00^{+0.02}_{-0.00}$	1.02 ± 0.01	$0.99^{+0.01}_{-0.03}$
$f(c \to D^0)$	0.99 ± 0.01	0.98 ± 0.01	$0.96^{+0.00}_{-0.02}$
$f(c \to D_s^+)$	$1.03^{+0.04}_{-0.06}$	$1.00^{+0.05}_{-0.03}$	$1.15^{+0.06}_{-0.05}$
$f(c \to \Lambda_c^+)$	$1.01^{+0.03}_{-0.05}$	$1.08^{+0.03}_{-0.02}$	$1.46^{+0.03}_{-0.09}$
$f(c \to D^{*+})$	$1.00^{+0.02}_{-0.03}$	$0.96^{+0.00}_{-0.02}$	$0.93^{+0.01}_{-0.02}$

Table 5: *The estimations of the extrapolation factors correcting charm fragmentation ratios and fractions measured in the accepted $p_T(D, \Lambda_c)$ and $\eta(D, \Lambda_c)$ region to those in the full phase space. The estimations were performed using three fragmentation schemes: the Peterson parameterisation of the charm fragmentation function as implemented in PYTHIA, the Bowler modification of the LUND symmetric fragmentation function as implemented in PYTHIA and the cluster model as implemented in HERWIG. The quoted uncertainties were obtained by varying relevant parameters in the PYTHIA and HERWIG MC generators.*

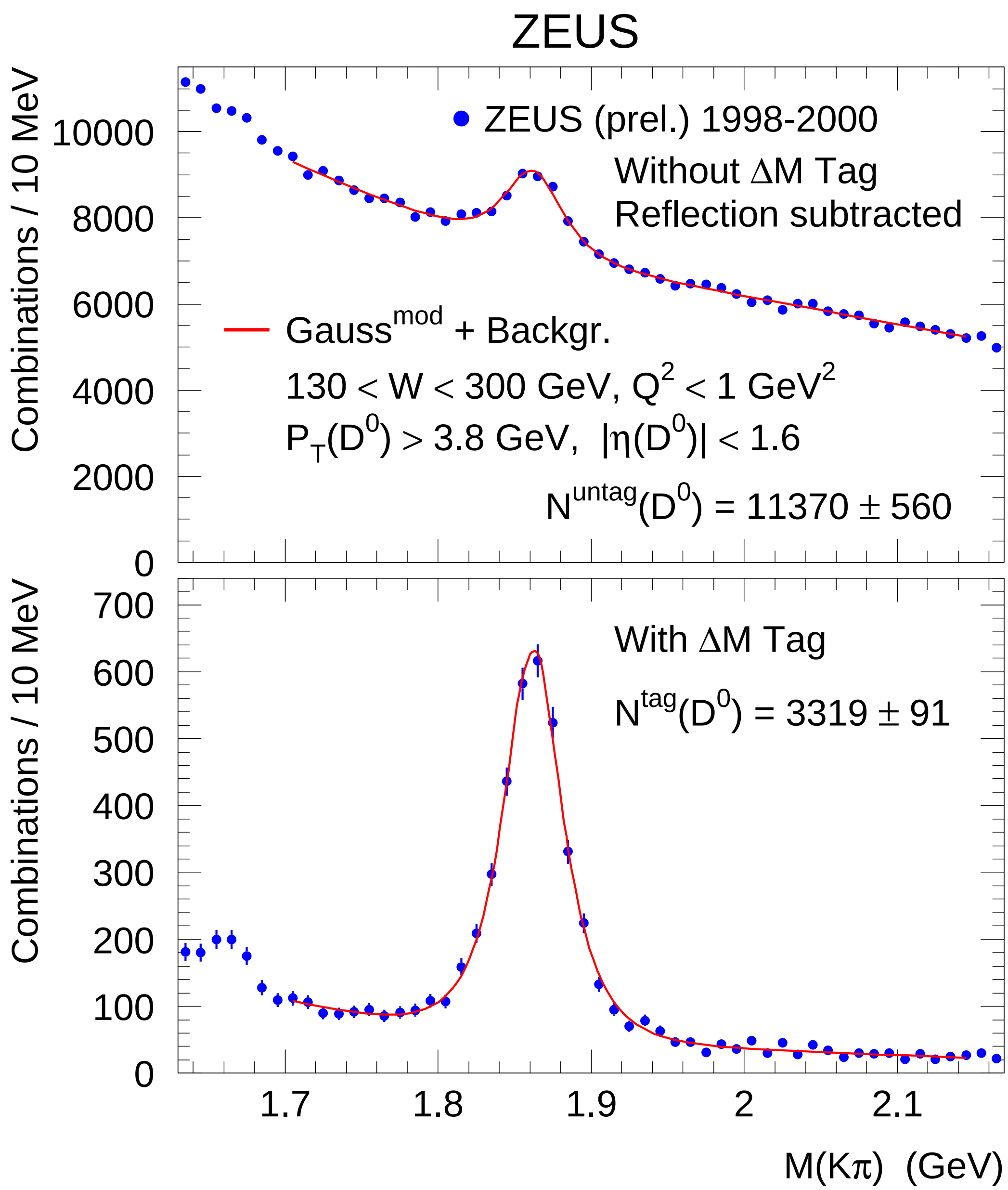

Figure 1: *The $M(K\pi)$ distributions for the D^0 candidates without ΔM tag, obtained after the reflection subtraction, and for the D^0 candidates with ΔM tag (dots). The solid curve represents a fit to the sum of a modified Gaussian function and a background function (see text).*

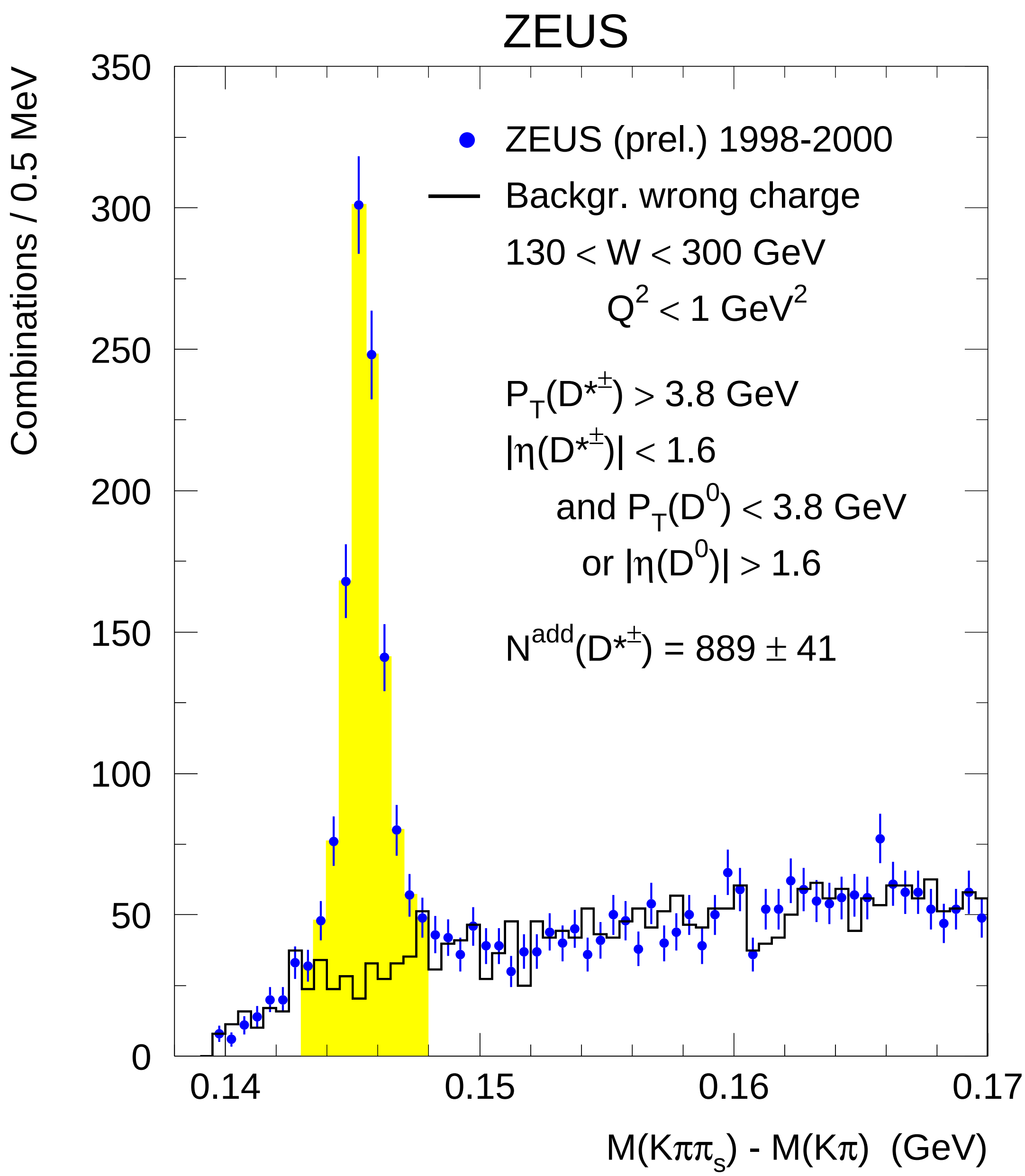

Figure 2: *The distribution of the mass difference, $\Delta M = M(K\pi\pi_s) - M(K\pi)$, for the "additional" $D^{*\pm}$ candidates (dots). The histogram shows the ΔM distribution for wrong charge combinations. The shaded band shows the signal range in which the wrong-charge background subtraction was performed (see text).*

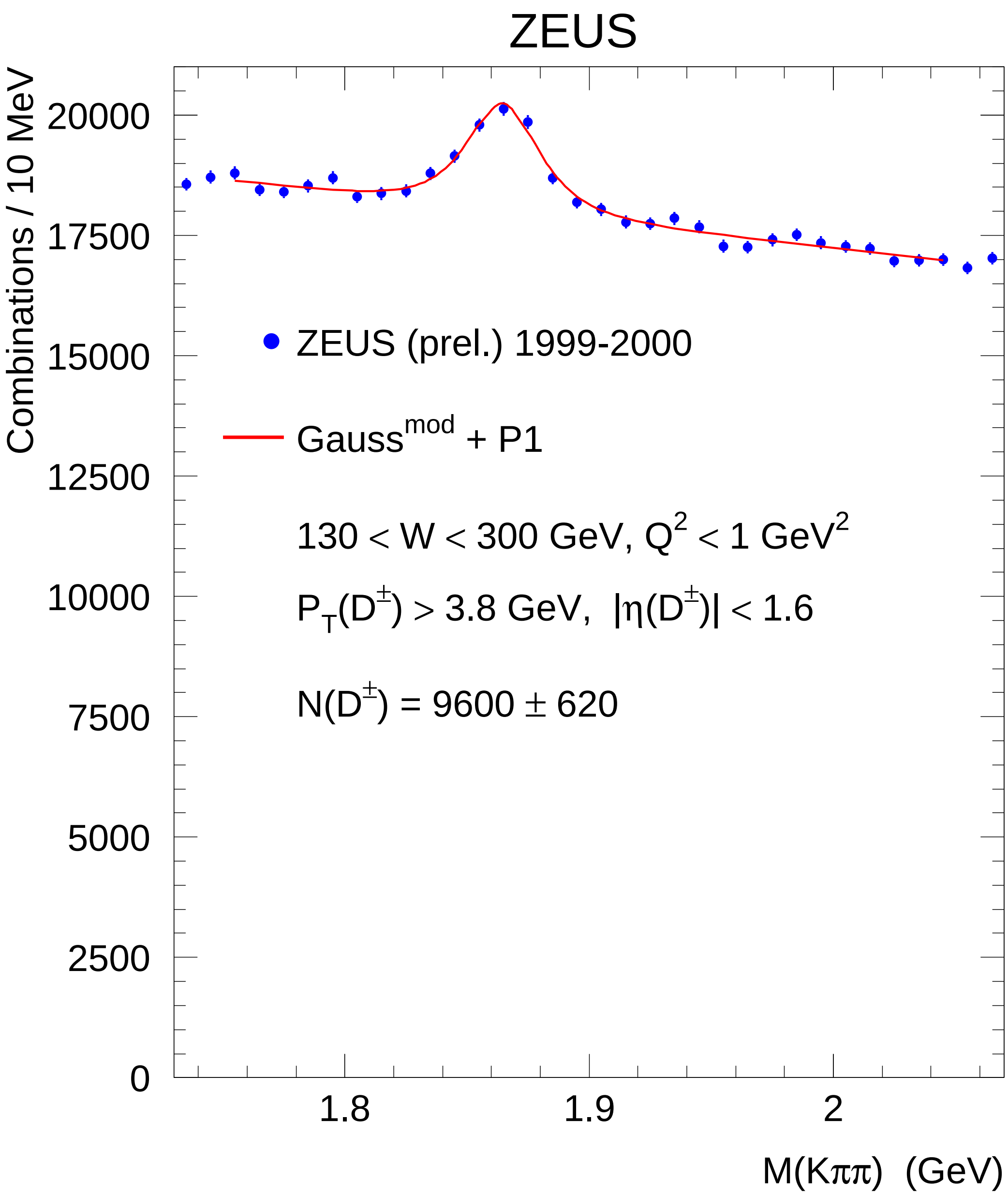

Figure 3: *The $M(K\pi\pi)$ distribution for the $D^{\pm}$ candidates (dots). The solid curve represents a fit to the sum of a modified Gaussian function and a linear background function (see text).*

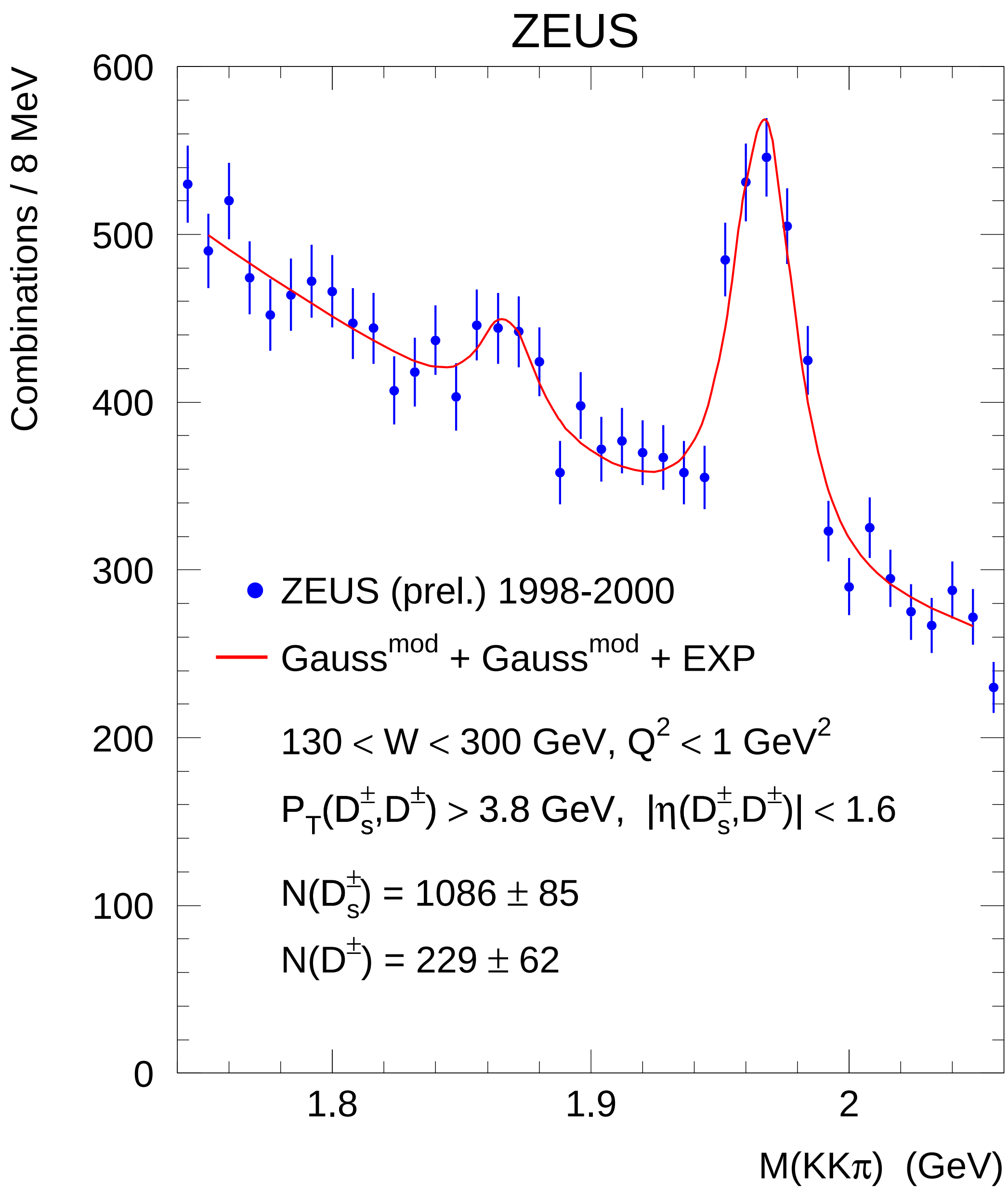

Figure 4: *The $M(KK\pi)$ distribution for the $D_s^{\pm}$ candidates (dots). The solid curve represents a fit to the sum of two modified Gaussian functions and an exponential background function (see text).*

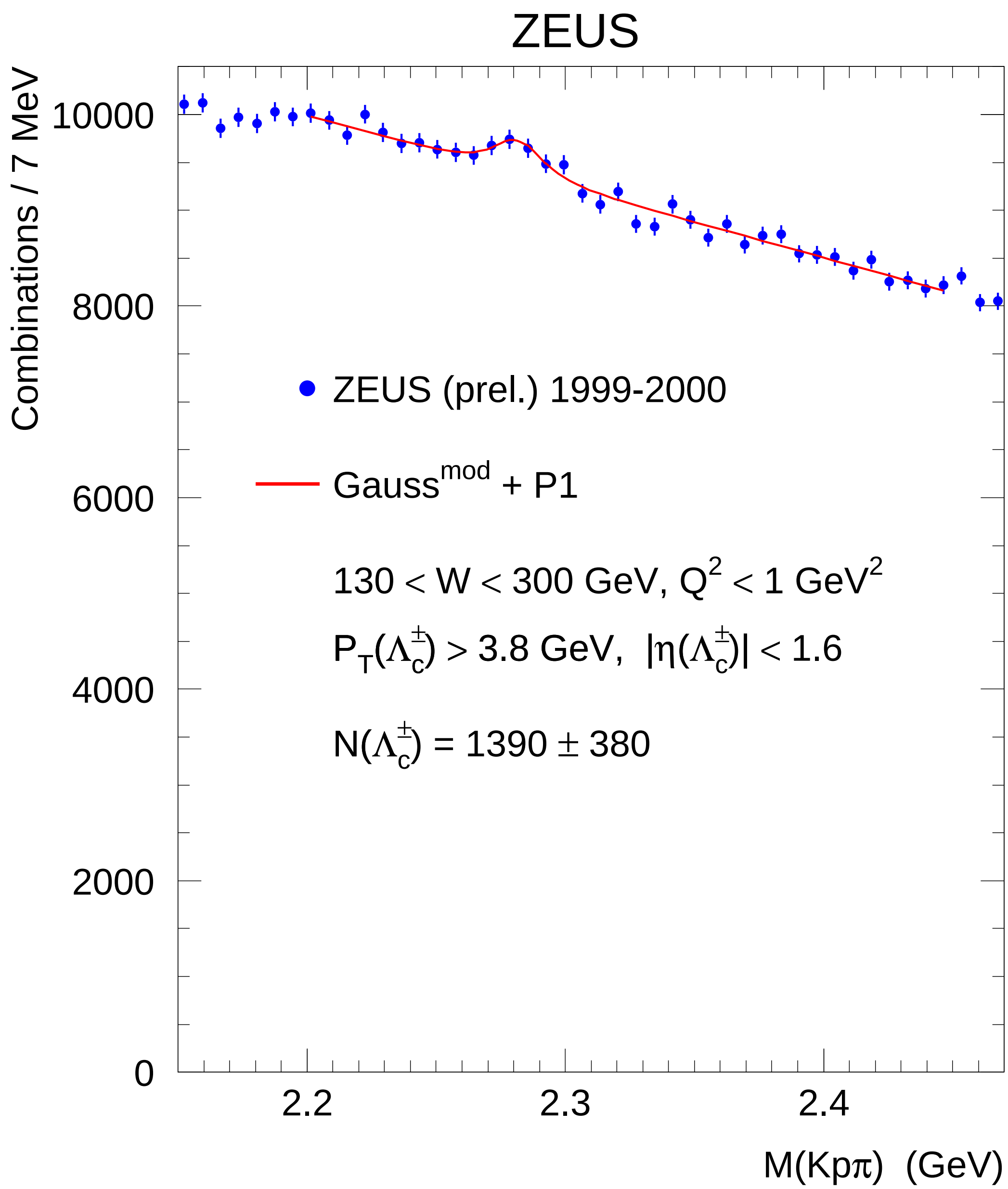

Figure 5: *The $M(Kp\pi)$ distribution for the $\Lambda_c^{\pm}$ candidates (dots). The solid curve represents a fit to the sum of a modified Gaussian function and a linear background function (see text).*